

Ramsey interference in one dimensional systems: The full distribution function of fringe contrast as a probe of many-body dynamics

Takuya Kitagawa,¹ Susanne Pielawa,¹ Adilet Imambekov,²
Jörg Schmiedmayer,³ Vladimir Gritsev,⁴ and Eugene Demler¹

¹*Physics Department, Harvard University, Cambridge, MA 02138, USA*

²*Department of Physics and Astronomy, Rice University, Houston, Texas 77005, USA*

³*Atominstytut, TU-Wien, Stadionallee 2, 1020 Vienna, Austria*

⁴*Physics Department, University of Fribourg, Chemin du Musée 3, 1700 Fribourg, Switzerland*

(Dated: November 6, 2018)

We theoretically analyze Ramsey interference experiments in one dimensional quasi-condensates and obtain explicit expressions for the time evolution of full distribution functions of fringe contrast. We show that distribution functions contain unique signatures of the many-body mechanism of decoherence. We argue that Ramsey interference experiments provide a powerful tool for analyzing strongly correlated nature of 1D interacting systems.

Introduction Recent progress in the field of ultracold atoms not only expanded our understanding of equilibrium properties of interacting 1d Bose gases [1, 2] but posed new theoretical challenges by studying far-from-equilibrium dynamics of such systems. Recent experiments addressed such questions as thermalization and integrability[3], decoherence after the splitting of two condensates[4] and spin dynamics of two component Bose mixtures[5]. Motivation for such experiments comes not only from the basic interests in many-body dynamics[6] but also from possible applications of ultracold atoms such as quantum information processing [7] and interferometric sensing[8]. In this paper we theoretically analyze the decoherence dynamics of Ramsey interference fringes in one dimensional quasi-condensates. Such systems have been considered for possible applications in atomic clocks and quantum enhanced metrology [9, 10]. In this paper we show that Ramsey interferometer is also a powerful tool for studying many-body dynamics of low dimensional quantum systems. We find that decoherence of Ramsey fringes is strongly affected by the multimode character of one dimensional systems. Moreover we will demonstrate that time evolution of the full distribution function of fringe contrast provides unique signatures of this many-body decoherence mechanism [11]. The idea of using noise and distribution functions to characterize equilibrium many-body states of ultracold atoms has been discussed in several theoretical papers [12] and applied in experiments[1, 13]. However there has been so far no application of this approach to non-equilibrium dynamics. This paper constitutes the first proposal to study non-equilibrium dynamics of ultracold atoms with quantum noise.

The role of interactions in Ramsey interferometers with BEC was first addressed in the pioneering paper of Kitagawa and Ueda[10]. They used single mode approximation to predict the interaction induced decoherence of Ramsey fringes along with the appearance of spin squeezed states. Their work stimulated ideas

for quantum-enhanced metrology that take advantage of spin squeezed states formed in interacting BECs [9, 14]. For the analysis of one dimensional quasi-condensates, however, the single mode approximation cannot be applied because these systems do not have macroscopic occupation of a single state even at zero temperature. The non mean-field character of the multi-mode spin dynamics in 1D quasi-condensates was first reported in the experiments of Widera et al [5]. However, this work did not provide the definitive demonstration of the many-body origin of decay. In the following, we argue that unambiguous signatures of the multimode decoherence are found in the full distribution function of the Ramsey fringe amplitudes. Such distribution functions should be accessible in experiments with 1D quasi-condensates realized on Atom Chips[15], because such systems do not average over multiple tubes and thus allow the measurements of shot-to-shot fluctuations [1].

Now we describe the Ramsey sequence considered in this paper. Here we identify two hyperfine states as spin up and down states. Ramsey sequence is carried out as follows: (i) all spins of the atoms are prepared in the spin up state; (ii) $\pi/2$ pulse is applied to rotate each spin into the x direction; (iii) spins freely evolve (precess) for time t ; (iv) another $\pi/2$ pulse is applied to map the transverse spin component to the z direction, which is then measured. Measurements yield a net spin \vec{S}_l for a segment of length l and we assume that l is smaller than the system size but large enough to contain large number of particles $N_l \gg 1$. In such a case, the simultaneous measurements of S_l^x and S_l^y are possible, because even though operators S_l^x and S_l^y generally do not commute, non-commutativity gives only corrections of the order of $1/\sqrt{N_l}$ relative to the average values [16]. Commutativity of S_l^x and S_l^y implies, in particular, that we can define the joint distribution function $P_l^{x,y}$ for the two transverse spin components S_l^x and S_l^y . In experiments, measurements of $P_l^{x,y}$ is possible by mapping the spin orientations in $x - y$ plane to z direction by $\pi/2$ pulse,

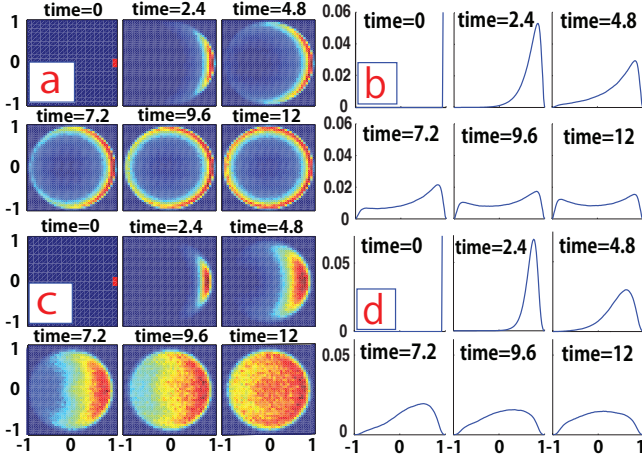


FIG. 1: (a),(c): Evolution of joint FDF $P_l^{x,y}$ with short integration length $l/\xi_s = 10$ (top, (a)) and long integration length $l/\xi_s = 30$ (bottom, (c)). (b),(d): Corresponding FDF for spin x , P_l^x with short integration length $l/\xi_s = 10$ (top, b)) and long integration length $l/\xi_s = 10$ (bottom, d)). Here $L/\xi_s = 200, K_s = 20$. Time is measured in units of ξ_s/c_s .

followed by local measurements of S_z [17]. S_l^x and S_l^y as well as the magnitude of spin $S_l^\perp = \sqrt{(S_l^x)^2 + (S_l^y)^2}$ can be found by taking the integration over l . The analytic solution for the time evolution of $P_l^{x,y}$ constitutes the main result of this paper. In addition, we assume that l is larger than the spin healing length ξ_s , so we can use Tomonaga-Luttinger liquid approach to describe the collective spin dynamics (see also below). For simplicity we work in the rotating frame of the Larmor precession, and consider the spins before the last $\pi/2$ pulse. Then the amplitude of Ramsey fringes, as it is conventionally defined, corresponds to S_l^x .

Our main results are summarized in Fig. 1 and can be understood from the following physical arguments. Strong fluctuations present in 1D systems forbid the existence of long range coherence[18], and spatial fluctuations coming from different wavelength strongly affect the dynamics in 1D. Among those, fluctuations with wavelengths longer than the integration length l rotate \vec{S}_l as a whole. So they decrease S_l^x but not the magnitude of the spin $S_l^\perp = \sqrt{(S_l^x)^2 + (S_l^y)^2}$. Fluctuations with wavelengths shorter than l decrease both S_l^x and S_l^\perp simultaneously. Fig.1 (a) (b) show the situation where fluctuations with wavelength larger than l dominate the dynamics. In (a), we see that the magnitude of the spin S_l^\perp decays only slightly from the initial state but the direction of the spin is randomized during the time evolution. Note that in this case the distribution function of S_l^x has a very peculiar shape with two peaks at large positive and negative values. We call this regime, "spin diffusion" regime. Fig.1 (c) (d) show the situation where fluctuations with wavelengths shorter than l dominate.

In this case S_l^\perp and S_l^x decay in the same timescale. We call this regime, "spin decay" regime. Below we argue that the crucial parameter of the system is a dimensionless ratio proportional to the length of the integration region $l_0 = \frac{\pi^2 l}{4K_s \xi_s}$. When $l_0 \leq 1$ the system is in the spin diffusion regime and the other limit $l_0 \gg 1$ is the spin decay regime.

Model. Following the first $\pi/2$ pulse we have a two component Bose mixture with equal densities of both species. Tomonaga-Luttinger liquid (TLL) approach, which we use in this paper, focuses on the linearly dispersing modes in the low energy part of the spectrum. For simplicity we consider the case when interaction parameters satisfy $g_{\downarrow\downarrow} = g_{\uparrow\uparrow}$ [21]. This condition can be reached for the hyperfine states $|F = 1, m_F = -1\rangle$ and $|F = 2, m_F = +1\rangle$ of ^{87}Rb that are commonly used in experiments [1, 5]. When this is the case, the charge and spin parts of the Tomonaga-Luttinger Hamiltonian decouple and the spin part of the Hamiltonian is given by

$$H_s = \frac{c_s}{2} \int_{-L/2}^{L/2} dr \left[\frac{K_s}{\pi} (\nabla \phi_s(r))^2 + \frac{\pi}{K_s} n_s^2(r) \right] \quad (1)$$

$$= \sum_{k \neq 0} c_s |k| b_{s,k}^\dagger b_{s,k} + \frac{c_s \pi}{2K_s} n_{s,0}^2, \quad (2)$$

Here L is the total system size, $n_s(r)$ describes the local spin imbalance (i.e. z component of the spin) $n_s = \psi_\alpha^\dagger (\frac{1}{2} \sigma_{\alpha\beta}^z) \psi_\beta$ and $n_{s,k}$ is the Fourier transform of $n_s(r)$. $\phi_s(r, t)$ describes the direction of the transverse spin component $\rho e^{i\phi_s} = \psi_\alpha^\dagger (\frac{1}{2} \sigma_{\alpha\beta}^+) \psi_\beta$ with ρ being the average density for each species. Variables n_s and ϕ_s obey canonical commutation relations $[n_s(r), \phi_s(r')] = -i\delta(r - r')$. K_s is spin Luttinger parameter representing the strength of interactions[5], and c_s is spin-wave velocity. Hamiltonian (2) has momentum cutoff set by the inverse of the spin healing length ξ_s^{-1} . In the weak interaction limit, these parameters are related to physical parameters as $c_s = \sqrt{g_s \rho / m}$, $\xi_s = \frac{\pi c_s}{g_s \rho}$ and $K_s = \xi_s \rho / 2$, where m is the mass of the particle and $g_s = \frac{4\pi^2 \hbar^2}{m} \frac{a_{\uparrow\uparrow} + a_{\downarrow\downarrow} - 2a_{\uparrow\downarrow}}{2}$ is the interaction strength in spin channel. In this paper, we focus on the regime $g_s > 0$ when the system is miscible. Our approach can be extended to $g_s < 0$ but will be limited to times before z magnetization per atom becomes of the order of one. The first and second term of (2) correspond to $k \neq 0$ and $k = 0$ part of the Hamiltonian, respectively. Here operators $b_{s,k}^\dagger$ create spin excitations with momentum k , and these spin excitations are the main focus of our study.

Transverse part of the spin operator \vec{S}_l is given by

$$S_l^x = \int_{-l/2}^{l/2} dr \rho \cos(\phi_s(r)), \quad S_l^y = \int_{-l/2}^{l/2} dr \rho \sin(\phi_s(r)), \quad (3)$$

When describing spin dynamics one typically considers time evolution of the expectation values $\langle S_l^a(t) \rangle$. However important information is also contained in the shot

to shot fluctuations of $S_l^a(t)$. Such quantum noise is captured by full distribution functions (FDF) of spin operators, $P_l^a(\alpha, t)$ [11]. In particular, high moments of $S_l^a(t)$ can be obtained from these FDFs $P_l^a(\alpha, t)$. Physically $P_l^a(\alpha, t)d\alpha$ is the probability that a single measurement of the spin operator S_l^a at time t gives the value between α and $\alpha + d\alpha$. In the experiments, $P_l^a(\alpha, t)$ can be obtained by making histograms of the measurement results of $S_l^a(t)$.

To describe time evolution of spin operators (3) we need to characterize the initial state of the system after the first $\pi/2$ rotation. The difficult part is translating the initial state of the microscopic language, where spins of all atoms pointing in the x direction, to the one in terms of the coarse grained degrees of freedom $\phi_s(r)$ and $n_s(r)$. Classically one expects the initial state to be the eigenstate of $\phi_s(r)$ with eigenvalue zero for all r . However such state is unphysical in quantum mechanics since it leads to infinite uncertainty of the conjugate variable $n_s(r)$, and thus, to infinite energy. More sensible initial state is a squeezed state of harmonic oscillator (1), which has reduced uncertainty in ϕ_s at the expense of enhanced fluctuations in n_s [5, 20]. To determine parameters of this state we observe that spins of individual atoms are independently rotated by the first $\pi/2$ pulse into x direction, so the initial state satisfies $\langle S^z(r)S^z(r') \rangle = \frac{\rho}{2}\delta(r - r')$. Thus we find a Gaussian state for the spin operator S^z in momentum space with fluctuations $\rho/2$ for all k :

$$|\psi_0\rangle = \frac{1}{\mathcal{N}} \exp\left(\sum_{k \neq 0} W_k b_{s,k}^\dagger b_{s,-k}^\dagger\right) |0\rangle |\psi_{s,k=0}\rangle, \quad (4)$$

where $2W_k = (1 - \alpha_k)/(1 + \alpha_k)$, $\alpha_k = |k|K_s/\pi\rho$ and \mathcal{N} is the overall normalization of the state. For the uniform part of the spin operator we also have a squeezed state $\langle n_{s,0} | \psi_{s,k=0} \rangle = \exp(-1/(2\rho)n_{s,0}^2)$. We note that model (1) has a short distance cut-off so the δ function in $\langle S^z(r)S^z(r') \rangle$ should be understood as rounded off on the scale of ξ_s , which is implicit in the momentum cut-off in Eq. (4).

Time evolution of the state (4) leads to $W_k \rightarrow W_k e^{2ic_s|k|t}$. From the resulting expression for the state at time t , one can readily calculate the decay of Ramsey fringes given by $\langle S_l^x(t) \rangle$, which is independent of integration length l (See also [5, 20]). To calculate time evolution of FDF, we define instantaneous annihilation operators $\gamma_{ks}(t)$ such that application of $\gamma_{ks}(t)$ on the state $\exp\left(W_k e^{2ic_s|k|t} b_{s,k}^\dagger b_{s,-k}^\dagger\right) |0\rangle$ gives zero. Using operators $\gamma_{ks}(t)$, one can apply the approach described in Refs. [1, 11] for calculating distribution functions of equi-

librium systems. After direct calculation we find [21]

$$P_l^{x,y}(\alpha, t) = \prod_k \int_{-\infty}^{\infty} e^{-\lambda_{rsk}^2/2} d\lambda_{rsk} \int_{-\pi}^{\pi} d\lambda_{\theta sk} \delta\left(\alpha - \rho \int_{-l/2}^{l/2} dr e^{i\chi(r,t,\{\lambda_{jsk}\})}\right), \quad (5)$$

$$\chi(r, t, \{\lambda_{jsk}\}) = \sum_k \lambda_{rsk} \sqrt{\frac{\langle |\phi_{s,k}(t)|^2 \rangle}{L}} \sin(kr + \lambda_{\theta sk}),$$

$$\langle |\phi_{s,k \neq 0}|^2 \rangle = \left(\frac{\pi\rho}{|k|K_s}\right)^2 \frac{\sin^2(c_s|k|t)}{2\rho} + \frac{\cos^2(c_s|k|t)}{2\rho},$$

$$\langle |\phi_{s,k=0}|^2 \rangle = \frac{1}{2\rho} + \left(\frac{c_s\pi t}{K_s}\right)^2 \frac{\rho}{2}, \quad (6)$$

where the real and imaginary part of α corresponds to x and y component of \vec{S}_l , respectively. Eq. (5), (6) allow a simple physical interpretation. Function $\chi(r, t, \{\lambda\})$ defines the local direction of transverse magnetization, which results from the summation over spin-wave like modes $\sin(kr + \lambda_{\theta sk})$. Amplitudes of individual modes are given by the time dependent expectation values $\langle |\phi_{s,k}(t)|^2 \rangle$ and by the set of random variables λ_{rsk} drawn from a Gaussian ensemble. Eq. (5), (6) reflect the key feature of dynamics of the quadratic Luttinger model (1): initial Gaussian state for $\phi_{s,k}$ remains Gaussian at all times [19].

Time evolution of $\langle |\phi_{s,k}(t)|^2 \rangle$ following the first $\pi/2$ rotation can be understood as free dynamics of a harmonic oscillator. From the conjugate nature of $\phi_{s,k}$ and $n_{s,k}$ we find $\langle |\phi_{s,k}(0)|^2 \rangle = \frac{1}{4} \frac{1}{\langle n_{s,k}(0)|^2 \rangle} = \frac{1}{2\rho}$ at $t = 0$. Subsequently $\langle |\phi_{s,k}(t)|^2 \rangle$ oscillates between the minimal value in the initial state and some maximum value $\langle |\phi_{s,k}|^2 \rangle_{max}$ at the frequency of a harmonic oscillator $c_s|k|$. $\langle |\phi_{s,k}|^2 \rangle_{max}$ can be estimated from energy conservation. Since the initial state was squeezed with respect to ϕ_{sk} , most of the energy of the mode is stored in the interaction term $|n_{s,k}|^2$. Therefore the total energy of the harmonic oscillator for momentum k can be approximated by $\frac{\pi c_s \rho}{K_s}$, which in turn gives $\langle |\phi_{s,k}|^2 \rangle_{max} \sim \frac{2\pi^2 \rho}{K_s^2 k^2} = \frac{1}{2\rho} \left(\frac{\pi\rho}{|k|K_s}\right)^2$. These considerations lead to the dynamics of phase fluctuation amplitude of the form in (6). We note that the spin fluctuations are dominated by small momentum since the maximum fluctuation amplitude is suppressed as $1/k^2$ for large momentum. This justifies our analysis based on the Tomonaga-Luttinger theory.

Results of numerical plots based on Eq. (5), (6) are shown in Fig. 1. In Fig. 2 (a) we also present the distribution function P_l^\perp of the magnitude square of the integrated spin $(S_l^\perp)^2$, which clearly demonstrates the difference between the "spin diffusion" and "spin decay" regimes. The character of these distribution functions

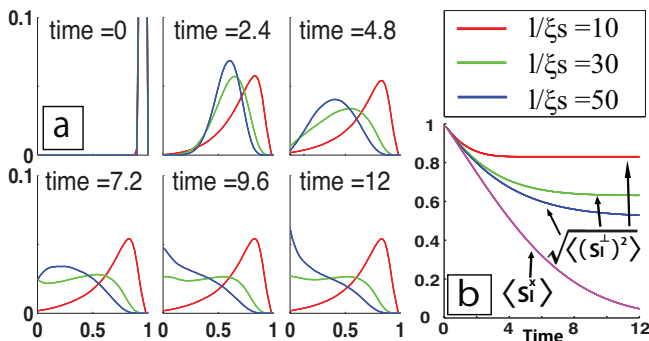


FIG. 2: (a): Time evolution of the distribution P_l^\perp for the magnitude of spin $(S_l^\perp)^2$. (b): time evolution of $\langle S_l^\perp \rangle$ and $\sqrt{\langle (S_l^\perp)^2 \rangle}$ with various integration length $l/\xi_s = 10, 30, 50$. Here we set $K_s = 20$, $L/\xi_s = 200$.

can be understood from the following arguments. We first discuss the "spin diffusion" regime, where the characteristic wavelength of spin fluctuations is longer than the integration length l (Fig. 1 (a), (b)). In this regime, all spins within l essentially point in the same direction and S_l^\perp remains large even after a long time evolution. Thus we find a peak at $(S_l^\perp)^2 \approx 1$ in the distribution function P_l^\perp (red line). In the other regime of "spin decay" (Fig. 1 (c), (d)), the typical length scale of spin fluctuations is shorter than the integration length l . In this case integration of spins over l is akin to taking a random walk in 2D plane and accordingly, distribution for $(S_l^\perp)^2$ approaches exponential form with a peak at $(S_l^\perp)^2 = 0$ in P_l^\perp (blue line). In the intermediate regime, we observe two peak structure for P_l^\perp , where the distribution exhibits both characteristic peaks (green line). We can understand the condition that separates these "spin decay" and "spin diffusion" type dynamics in the following way. Deviation of spin angles at $r = l$ relative to $r = 0$ can be estimated from $\Delta\chi \approx \frac{1}{\sqrt{L}} \sum_k \lambda_{rsk} \sqrt{\langle |\phi_{s,k}|^2 \rangle_{max}} \sin(kl)$. A typical magnitude of $\Delta\chi$ is given by $\langle (\Delta\chi)^2 \rangle$ where the average is taken over fluctuations of λ_{rsk} . The factor $\sin(kl)$ in $\Delta\chi$ effectively limits momentum integration range to $k > 2\pi/l$, so $\langle (\Delta\chi)^2 \rangle \approx \frac{\pi^2 l}{2K_s \xi_s}$. When $\langle (\Delta\chi)^2 \rangle^{1/2}$ is smaller than 2π the system is in the "spin diffusion" regime. When $\langle (\Delta\chi)^2 \rangle^{1/2}$ becomes of the order of 2π and larger, the system enters the "spin decay" regime. The crossover takes place around $\frac{\pi^2 l}{4K_s \xi_s} \sim 1$.

In the "spin diffusion" regime, the dynamics of S_l^\perp and S_l^x display different time scales as can be seen in Fig. 2 (b). In order to understand this separation of time scale, we note that the magnitude of the integrated spin S_l^\perp is only affected by fluctuations with short wavelengths, $\lambda < l$, for which dynamics takes place at short time scale. Hence $\langle S_l^\perp \rangle$ decays until the time $t_\perp \approx 2\pi l/c_s$ (see Eq. (6)) and then it reaches a saturated value. On the other

hand S_l^x is affected by excitations of all wavelength, so $\langle S_l^x \rangle$ decays until it reaches 0. These behaviors are shown in Fig. 2 (b), where we compared the decay of $\langle S_l^\perp \rangle$ for various segment length l and $\langle S_l^x \rangle$.

Non-trivial time evolution of the distribution functions P_l^x , $P_l^{x,y}$ and especially the striking contrast of the "spin diffusion" and "spin decay" regimes should provide unique signatures of the non-mean-field character and multimode dynamics of 1D systems.

Before concluding this paper we point out that our analysis can be extended to the problem of splitting a single 1D quasi-condensate into two, as it was done with an RF potential in experiments reported in Refs.[4]. While earlier theoretical work focused on the time decay of the average fringe contrast[20], the method developed in this paper can be used to study the time evolution of the full distribution function.

Summary. We provided theoretical analysis of Ramsey interference experiments with one dimensional quasi-condensates. We discussed time evolution of the full distribution functions of fringe contrast and showed that they contain unique signatures of the many-body dynamics of one dimensional systems. This work was supported by the NSF grant DMR-0705472, Harvard MIT CUA, DARPA OLE program, AFOSR MURI, and Swiss NSF.

-
- [1] S.Hofferberth *et al.*, Nature Physics 4, 489 (2008).
 - [2] B. Paredes *et al.*, Nature 429, 277(2004); T. Kinoshita, T. Wenger, D. S. Weiss, Science 305 30 (2004); A. H. van Amerongen, *et al.*, Phys. Rev. Lett. 100, 090402 (2008).
 - [3] T.Kinoshita, T.Wegner, D. Weiss, Nature 440, 900 (2006).
 - [4] S.Hofferberth *et al.*, Nature 449, 324 (2007).
 - [5] A.Widera *et al.*, Phys. Rev. Lett. 100, 140401 (2008).
 - [6] I. Shvarchuck *et al.*, Phys. Rev. Lett. 89, 270404 (2002); P. Calabrese, J.S. Caux, Phys. Rev. Lett. 98, 150403 (2007); M. A. Cazalilla, J. B. Marston, Phys. Rev. Lett. 88, 256403 (2002); M. Rigol, V. Dunjko, and M. Olshanii, Nature 452, 854(2008); E.Altman *et al.*, Phys. Rev. Lett. 95, 020402 (2005); A. Polkovnikov and V. Gritsev, Nature Physics 4, 477 (2008); U. Schollwöck, Rev.Mod.Phys. 77, 1, 259 (2005).
 - [7] T. Calarco *et al.*, Phys. Rev. A 61, 022304 (2000).
 - [8] A. D. Cronin, J.Schmiedmayer, D. E. Pritchard Rev. Mod. Phys. 81, 1051 (2009).
 - [9] A.S. Sorensen, K. Molmer, Phys.Rev.Lett. 83,2274 (1999); A.Sorensen *et al.*, Nature 409, 63 (2001).
 - [10] M.Kitagawa,M.Ueda, Phys. Rev. A 47, 5138(1993).
 - [11] A. Polkovnikov, E. Altman, E. Demler, PNAS, 103:6125 (2006); A. Imambekov, V. Gritsev, E. Demler, Phys.Rev.A, 77, 063606 (2008); V. Gritsev *et al.*, Nature Physics 2:705 (2006).
 - [12] E. Altman, E. Demler, M. D. Lukin, Phys. Rev. A 70:013603 (2004); K. Eckert *et al.*, Nature Physics 4, 50 (2008); A. Lamacraft, Phys. Rev. A 76, 011603(R) (2007).
 - [13] Z. Hadzibabic *et al.*, Nature 441, 1118 (2006).

- [14] A.M.Rey *et al.*, Phys. Rev. A 77, 052305 (2008).
- [15] R. Folman *et al.*, Phys.Rev.Lett. 84, 4749 (2000); R.Folman *et al.*, Adv.At.Mol.Phys. 48, 263 (2002); J.Fortagh and C.Zimmermann, Rev. Mod.Phys. 79, 23 (2007).
- [16] A. Polkovnikov, Europhys. Lett. 78, 10006 (2007).
- [17] G.B.Jo *et al.*, Science 18, 325.5947, 1521(2009).
- [18] T. Giamarchi: Quantum Physics in One Dimension (Oxford University Press, Oxford, U.K., 2004).
- [19] Temperature determines the density fluctuations before the $\pi/2$ spin rotation. However, spin and density fluctuations are decoupled in the system we consider so that our results do not depend on temperature. Corrections due to small $g_{\uparrow\uparrow} \neq g_{\downarrow\downarrow}$ introduce temperature dependence, but they do not lead to qualitative changes [21].
- [20] R.Bistritzer, E. Altman, PNAS 104, 9955 (2007); A.A. Burkov, M.D. Lukin, E. Demler, Phys.Rev. Lett. 98:200404 (2007); I.E. Mazets, J. Schmiedmayer, Euro. Phys. J. B (2009).
- [21] T.Kitagawa *et al.*, in preparation.